

Photoluminescence Studies and Core–Shell Model Approach for Rare Earthdoped CdWO₄ Nano Phosphor

M. Srinivas · Dhaval Modi · Nimesh Patel ·
V. Verma · K. V. R. Murthy

Received: 29 June 2014 / Accepted: 13 August 2014 / Published online: 27 August 2014
© Springer Science+Business Media New York 2014

Abstract The present paper reports synthesis and photoluminescence studies of Cadmium tungstate (CdWO₄) and Cerium doped CdWO₄. The phosphor samples were synthesized by low cost and low temperature hydrothermal method. The received materials are characterized by XRD, FTIR, TEM and photoluminescence (PL) studies are reported. XRD pattern reveals that the CdWO₄ has monoclinic wolframite structure and the shift toward higher angle of reflection peaks suggests that the cell parameters of as-synthesized phosphor could continuously decrease and also crystallite size decreases when the Ce concentration increases. The FTIR spectrum of Cerium doped CdWO₄ exhibits intrinsic bending (Cd-O) and stretching vibrations (W-O). When the pH is varied from 4 to 8 the formation of nano spheres (4 pH) nano rods (6 pH) and agglomeration as well as nano tubes (8 pH) are observed which are confirmed from TEM studies. This may be due to that formation of nano material and also the change in nature of aqueous solution from acidic to basic. When the pH changed from acidic to basic while preparing the materials the observed PL emission in the synthesized phosphor the PL intensity increases. From PL studies it suggests that more radiative traps are responsible in basic medium when compare to acidic solution and 7 nm shift in PL emission spectra observed (blue to violet region) may be due the formation of nano phosphor.

Keywords CdWO₄ · Hydrothermal method · pH · Nano particle · Photoluminescence

1 Introduction

Metal tungstates have been good application prospects in scintillators, optical fibers, microwave applications, humidity sensors, photoluminescence materials etc., [1–4]. Cadmium tungstate (CdWO₄) have been investigated for many applications, such as, oil well logging, industrial processing control and inspection, dosimetry, and nuclear weapons and waste monitoring [5–9]. CdWO₄ with a monoclinic wolframite structure is a highly functional material due to its low radiation damage, low afterglow to luminescence, high average refractive index, high density (7.9 g/cm³), and high X-ray absorption coefficient [10]. It is also has potential use as an advanced medical X-ray detector in computerized tomography [11] has attracted interest of many researchers.

Hydrothermal synthesis of these materials by the synthetic route is a simple and cost effective method that provides a high yield with easy scale up, and is emerging as a viable alternative approach for the synthesis of inorganic materials with appropriate choice of experimental parameters, such as temperature, time, pH, mineralizer and surfactant. It offers several advantages over other synthesis process, such as mild experimental conditions, high purity, and good particle size distribution of product.

The tungstate doped with rare-earth nanophosphors have attracted special attention compared to the corresponding bulk materials have large practical applications in solid state lighting and displays. In the present work, we report the synthesis of cerium doped CdWO₄ by hydrothermal method. It is noticed that the pH of solution has an essential

M. Srinivas · D. Modi (✉) · N. Patel · V. Verma
Faculty of Science, Physics Department, The Maharaja Sayajirao
University of Baroda, Vadodara 390002, Gujarat, India
e-mail: bgjdmodi@gmail.com

K. V. R. Murthy
Faculty of Technology and Engineering, Applied Physics
Department, The Maharaja Sayajirao University of Baroda,
Vadodara 390001, Gujarat, India

role in crystal growth under hydrothermal conditions [12, 13]. Liao et al. [14] examined the effect of the wide pH of synthesizing solution on the formation of CdWO_4 nanorods and reported an optimal range of the initial pH value to be 3–8. Recently, Mirabbos et al. [15] investigated the effect of the pH of synthesizing solution on the formation of besom-like CdWO_4 structures. In the present study, we report the effect of the pH on the PL studies, different morphology and other properties of Ce doped CdWO_4 .

2 Experimental Details

2.1 Sample Preparation

Cadmium Chloride ($\text{CdCl}_2 \cdot \text{H}_2\text{O}$), sodium tungstate ($\text{Na}_2\text{WO}_4 \cdot 2\text{H}_2\text{O}$) and cerium oxide (CeO_2) analytical grade was used as received without any further purification purchased from Alfa Aesar. Distilled water was used as a solvent to prepare all required solutions used in the present investigations. Initially 40 ml solution of 0.1 M concentration of $\text{CdCl}_2 \cdot \text{H}_2\text{O}$ was prepared by continuous stirring and also 40 ml solution of 0.1 M concentration of $\text{Na}_2\text{WO}_4 \cdot 2\text{H}_2\text{O}$ was added into it drop wise subsequently 40 ml solution of 0.01 M concentration of CeO_2 was added. The pH value 4, 6, 8 of this solution was adjusted drop wise with CH_3COOH or NaOH solution. This prepared solution of pH 4, 6 and 8 are denoted as sample a, b and c respectively. These precursors solutions (sample a, sample b and sample c) were transferred to teflon-lined stainless-steel autoclaves having 150 ml capacity filled with reaction media up to 80 % one by one. The autoclave was maintained at a temperature of 150 °C for 12 h and allowed to cool to room temperature. The prepared samples were washed several times with distilled water and lastly washed with absolute ethanol. Finally, a white powder was obtained after drying in vacuum at 80 °C for 2 h.

2.2 Characterization

The XRD measurements were carried out with Japan Rigaku D/max X-ray diffractometer, using Ni-filtered $\text{Cu K}\alpha$ radiation. A scan rate of 0.5°/s was applied to record the patterns in the 2θ range 10–70°. FTIR spectra recorded on a Jasco FTIR-4100, spectrophotometer (Japan) by mixing with KBr in mortar and pestle in the ratio of 1:10. The nanostructure and surface morphology of the CdWO_4 were observed by transmission electron microscopy (TEM, Tecnai 20 G2 FEI made). The PL of the samples was investigated on a Shimadzu 1503R spectrofluorophotometer at room temperature with a xenon lamp as excitation source.

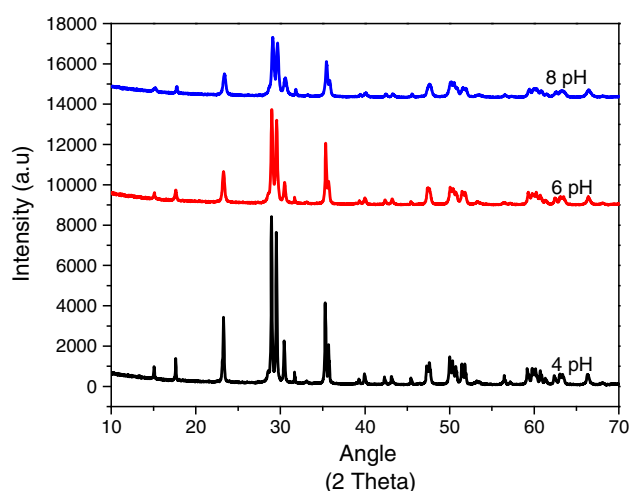


Fig. 1 XRD patterns of cerium doped CdWO_4 synthesized at different pH (4, 6, 8)

3 Results and Discussion

3.1 XRD

Figure 1 shows the XRD patterns of CdWO_4 :Ce powders prepared at different pH (4, 6, 8). XRD patterns revealed that the CdWO_4 can be indexed to a pure monoclinic phase of CdWO_4 with a wolframite structure with space group $\text{P2}/c$ (13); in agreement with JCPDS (Joint Committee on Powder Diffraction Standards) card No. 14-0676. It can be seen that the crystal structures of all the samples belong to the pure monoclinic phase. However, on comparing the curves of the three products, it is observed that the relative intensity of the peaks varied considerably, which indicates different crystallinity. The samples prepared at pH 4 and 6 show better crystallization than the one made at pH 8. The broadening of the peaks indicates that the crystallite size is small. These XRD patterns indicate that well-crystallized CdWO_4 crystals were observed in the current synthetic process. This result shows that different pH supports the formation of crystalline CdWO_4 nanostructures at low synthesis temperature therefore reduces the processing time than other conventional methods.

Shift in the main reflection peak of CdWO_4 is compared and presented in Fig. 2. It can be seen from the figure that peak when sample prepared at pH 4 is at lowest angle and that for sample prepared at pH 8 is at highest angle. According to the Bragg equation, the shift toward higher angle of reflection suggests that the cell parameters of as-synthesized products could continuously decrease and also crystallite size decreases.

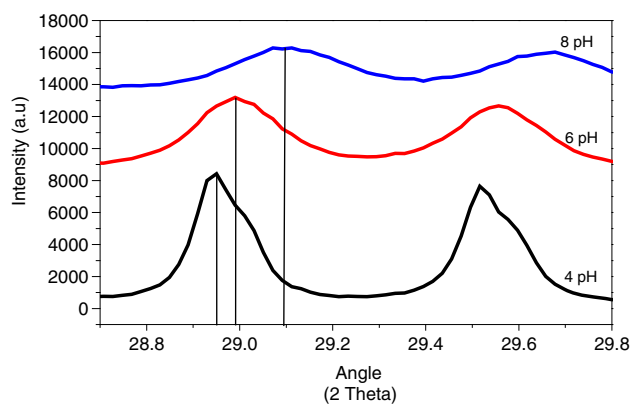


Fig. 2 Shift of reflection peak of cerium doped CdWO₄ synthesized at different pH (4, 6, 8)

Table 1 Lattice parameters and average crystallite size

pH	Lattice parameters (nm)			Avg crystallite size (nm)
	a	b	c	
4	5.0240	5.865	5.0860	55
6	5.0280	5.8620	5.0670	47
8	5.0110	5.8040	5.0500	44

The summary of lattice parameters and average crystallite size calculated using the Scherrer formula are given Table 1.

$$D = \frac{k\lambda}{\beta \cos \theta}$$

where D is the average crystallite size, k is the constant equal to 0.89, λ is the wavelength of the X-rays equal to 0.1542 nm and β is FWHM.

3.2 FTIR Studies

Figure 3 shows FTIR spectra recorded in the range of 1,600–400 cm^{-1} of the cerium doped CdWO₄ particles. FTIR measurements were done using KBr method at room temperature. The intrinsic bending and stretching vibrations of Cd–O (517, 560 cm^{-1}), W–O ($\sim 680 \text{ cm}^{-1}$) and Cd–O–W ($\sim 824 \text{ cm}^{-1}$) were observed in the all three samples. The FTIR spectrum of all samples exhibit broad band below 710 cm^{-1} which is due to the δ (Ce–O–C) mode [16]. The band observed at 3,410–3,450 cm^{-1} may be attributed to O–H stretching mode of water which is due to absorbed water molecules on sample surfaces and the band centered at 1,630 cm^{-1} is associated with the deformation vibration for H–O–H bonds of water. Residual water and hydroxy groups are usually detected in the as

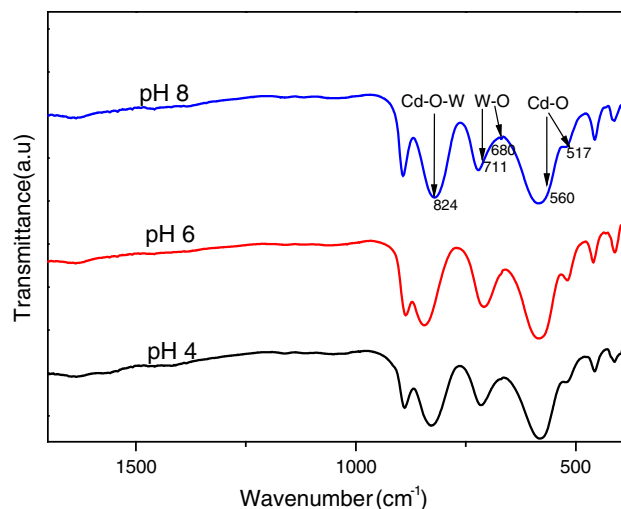


Fig. 3 Room temperature FTIR spectra of cerium doped CdWO₄ synthesized at different pH (4, 6, 8)

synthesized samples regardless of method used [17] and further heat treatment is necessary for their elimination.

3.3 Transmission Electron Microscopy [TEM]

Figure 4 display TEM images of cerium-doped samples of the CdWO₄ prepared at 150 °C for 12 h. The TEM image shows nano spheres when pH maintained at 4. The average diameter of nano sphere is around 110–150 nm. It exhibits distinct boundaries of nanospheres formed and are seen quite smooth. The nano spheres distributed homogenously from pH 4 specimen.

When the pH maintained at 6, 1-dimensional nano rods have been observed from TEM study. It is seen from the figure that all CdWO₄ nano rods are self-assembled. From the TEM figure the length of the nanorod is around 70–120 nm and the width is about 50 nm for pH 6 material.

From TEM for pH 8 material we found agglomerated particles and also hollow nanotubes. Hollow nanotubes have an average outer diameter of about 10–20 nm and their length increases from 50–300 nm. From TEM for pH 8 material the shape of the particles is not perfectly spherical and also having non uniform rough surface along with nano halo tubes. Because of the small diameter, these nanotubes have tendency to bundle together, this phenomenon always observed in single walled carbon nanotubes. A sharp observation of the nanotubes reveals that they have a narrow width distribution and identical inner and outer diameter throughout their entire length.

Construction of hollow nanotubes in our case can be explained on the basis of Kirkendall counter diffusion effect. In this effect two solutions CdCl₂ (solution A) and

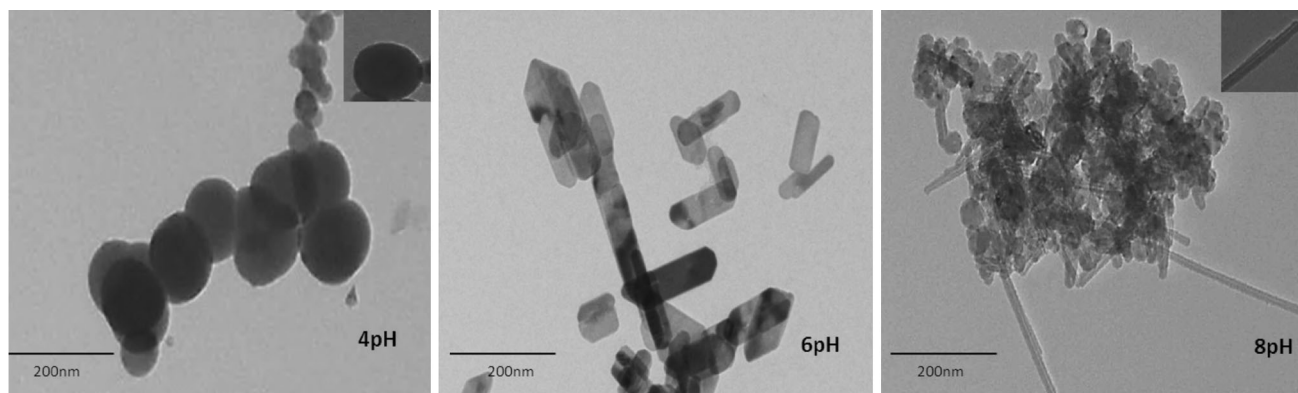


Fig. 4 TEM images of cerium doped CdWO_4 synthesized at different pH (4, 6, 8)

Na_2WO_4 (solution B) sacrifice themselves to produce hollow nano tube of CdWO_4 (solution AB). We proposed that there are two possible approaches which are named as *Approach A* and *Approach B*. Both possibilities are based on Core/Shell model with difference only in Core and Shell Compound [18]. Approach A is shown schematically in Fig. 5. The approach A can be explained as following steps:

- (I) The mechanism initiates when pH is 8.
- (II) It is expected that when pH is maintained at 8, CdCl_2 molecule behaves as a Core and Na_2WO_4 molecule gathered around it and forms a shell.
- (III) Cd^{2+} ion from the core diffuse to the shell side and WO_4^{2-} ion from the shell diffuse towards the core side. At the same time small isotropic voids will form in core contains only Cl^- ions. By this way Kirkendall diffusion will takes place in the form of two ways and corresponding mass will exchange (Wagner counter diffusion) between core and shell compounds. Thus, the product CdWO_4 forms at the edge of the core/shell interface site. Simultaneously, Na^+ move and react with Cl^- at outer side to form NaCl which may be dissolved in generated aqueous solution.
- (IV) Small voids fuse into each other and forms larger voids.
- (V) By this approach, hollow nano tubes will be produced with larger cavity.

Hollow nano tube of CdWO_4 may also be formed via Approach B which is in a similar way by considering Na_2WO_4 as Core and CdCl_2 as Shell.

The main formation of hollow nano tube is due to the change in nature of aqueous solution from acidic to basic where the pH was changed from 4 to 8. The mechanism of the CdWO_4 nanorods through hydrothermal approach shows that the growth process is not assisted by surfactant or template-directed, As no surfactants or templates are

introduced into the synthesis process, it is confirmed from our result, that the increase in pH affects the corresponding change in size of CdWO_4 nanoparticles as well as length of the CdWO_4 nanotubes and nanorods.

3.4 Photoluminescence (PL) Studies

The excitation spectra of Ce doped CdWO_4 phosphors recorded at room temperature is shown in Fig. 6 when monitored at 470 nm. Broad absorption band is observed between 240 and 320 nm. The absorption intensity of the broad band centered around 270 nm increases when the pH increases from 4 to 8. The intensity is more than 50 % increase when compared pH 8 to 4.

The PL spectra of the Cerium doped CdWO_4 synthesized at different pH are shown in Fig. 7. It is clearly seen that, the PL emission band (380–600 nm) with intense emission (469 and 476 nm) are identical in all three spectra. The low intensity peaks at 368 nm; in near-UV region is also observed in all three spectra. The results indicate that PL spectra exhibit violet–green emission band peaking in blue region with a band edge UV emission. The emission bands were ascribed to the $^1\text{A}_1 \rightarrow ^3\text{T}_1$ transition within the WO_6^{6-} complex [19]. This is mainly due to the charge-transfer transitions between the O_{2p} orbital and the empty d orbital of the central W^{6+} of WO_6 octahedra or to the self-trapped exciton at a WO_6^{6-} oxyanion complex [20, 21]. The band edge UV emission may be due to recombination of free excitons through in exciton–exciton collision process or the radiative recombination of excitons bound to neutral donor [22, 23]. The change in PL intensity can be attributed to change in dimensional confinement of Ce ions which is due to the preparation of the material through effective approach of pH.

The intensity of PL emission spectra increases with the increase in the pH of synthesizing solution this may be due to the formation of low dimension of the materials. This leads to availability of more number of particles for the

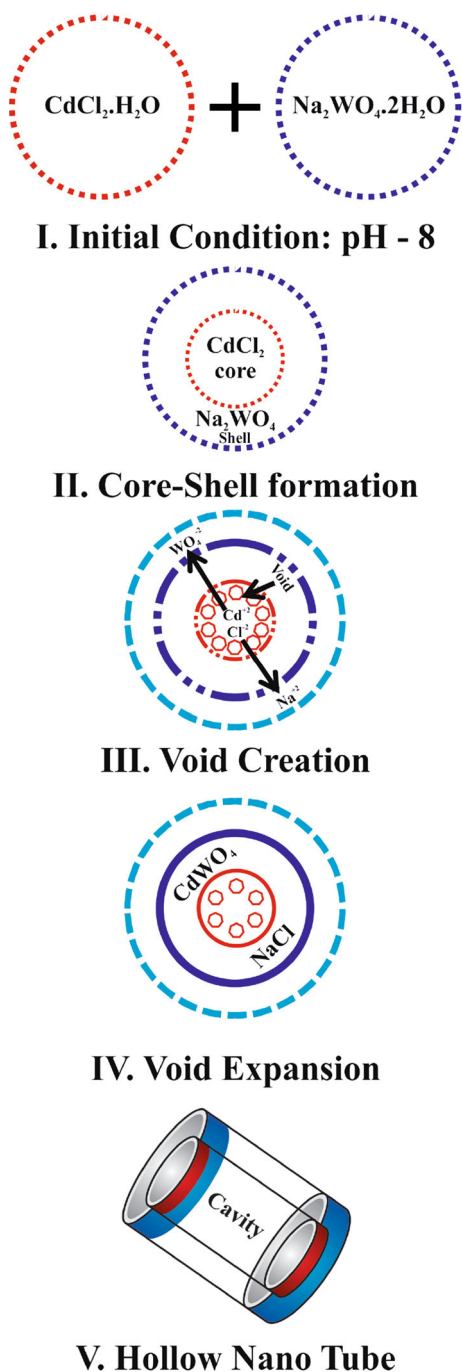


Fig. 5 Approach A for formation of hollow nano tube

formation of the excited electrons and hole pairs. This indicates that the PL intensity depends on the morphology as well as low dimension of the materials of CdWO₄ structures [24–26]. PL emission mainly originates from recombination of excited electrons and holes. Low PL emission intensity indicates that phosphor has a low recombination rate and high separation rate of electrons-holes as well as large particles in nano range. In the case of

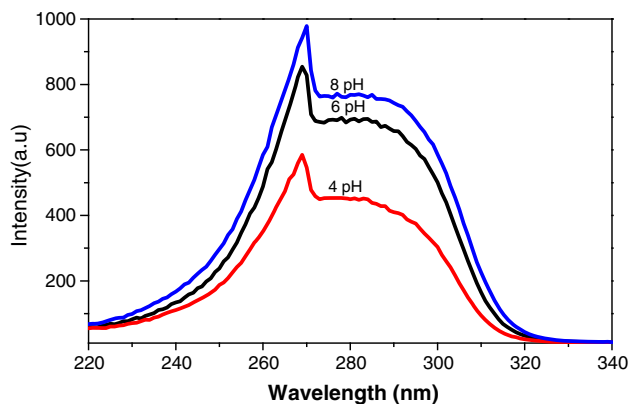


Fig. 6 Excitation spectra of cerium doped CdWO₄ synthesized at different pH (4, 6, 8) recorded with 475 nm emission wavelength

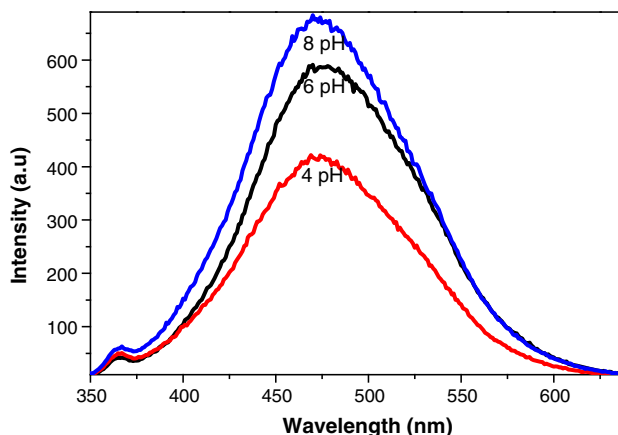


Fig. 7 PL emission spectra of cerium doped CdWO₄ synthesized at different pH (4, 6, 8) recorded with 270 nm excitation wavelength

Table 2 Peak positions with respect to pH

pH	Peak position (nm)	Peak intensity
4	476	421
6	476	586
8	469	683

pH 8, the high intensity peak is obtained due to high recombination rate and low separation rate between electrons and holes.

It is also observed from the Fig. 7 and Table 2 that there is a minor peak shift of 7 nm which is mainly responsible due to the medium in which occupation of Ce ions in the substitution positions of CdWO₄ host crystal lattice. From XRD to TEM measurements, it is inferred that all the samples have same phase. Therefore, the shifting of peak does not relate with phase and it is attributed to effect of

dopant in basic medium. The position of the peak changes in pH 8 solution compare to pH 4 and 6 solution and shift occurred from blue to violet region. In our earlier work [27] we reported the shift obtained due to dopant but in the present case the shift can be occurred due the formation of low dimensional particles in nano scale when compared to pH 4 materials mainly due to basic preparation medium.

4 Conclusion

Cerium doped CdWO_4 was successfully synthesized by hydrothermal process for pH 4, 6 and 8. XRD patterns reveal that the cell parameters of as-synthesized products could continuously decrease and also crystallite size decreases as pH increases. TEM images infer that pH affect the morphology of CdWO_4 in terms of its shape and size. PL emission studies shows broad intense peak at 469 and 476 nm wavelength in violet–green region peaking in blue region due the formation of low dimensional particles in nano scale. It suggest that more radiative traps generate in basic preparative medium when compare to acidic solution and shifting of peak is attributed to basic medium due the formation of low dimensional particles in nano scale.

Acknowledgments Author very thank full to UGC-DAE, Consortium for Scientific Research, Indore for XRD measurements.

References

1. S.J. Chen, J.H. Zhou, X.T. Chen, J. Li, L.-H. Li, J.-M. Hong, Z.L. Xue, X.-Z. You, *Chem. Phys. Lett.* **375**, 185 (2003)
2. S. Kwan, F. Kim, J. Akana, *Chem. Commun.* **447** (2001)
3. B. Liu, S.-H. Yu, F. Zhang, L.J. Li, Q. Zhang, L. Ren, K. Jiang, *J. Phys. Chem. B* **108**, 2788 (2004)
4. X.L. Hu, Y. Zhu, *J. Langmuir* **20**, 1521 (2004)
5. C.L. Melcher, R.A. Manentem, J.S. Schweitzer, *IEEE Trans. Nucl. Sci.* **36**, 1188 (1989)
6. C.L. Melcher, *Priv. Commun.* **75**, 75 (1994)
7. D. Brown, R.H. Olsher, Y. Eisen, J.F. Odriguez, *Nucl. Instrum. Methods Phys. Res. A* **373**, 139 (1996)
8. C.M. Bartle, R.C. Haight, *Nucl. Instrum. Methods Phys. Res. A* **422**, 54 (1999)
9. V. Ryzhikov, L. Nagornaya, V. Volkov, V. Chernikov, O. Zelenskaya, *Nucl. Instrum. Methods Phys. Res. A* **486**, 156 (2002)
10. H. Lotem, Z. Burshtein, *Opt. Lett.* **12** (1987)
11. C.D. Greskovich, D. Cusano, D. Hoffman, R.J. Riedner, *Am. Ceram. Soc. Bull.* **71**, 1120 (1992)
12. M. Hojamberdiev, G. Zhu, Y. Xu, *Mater. Res. Bull.* **45**, 1934–1940 (2010)
13. J. Wang, Y. Xu, M. Hojamberdiev, J. Peng, G. Zhu, *Mater. Sci. Eng., B* **156**, 42–47 (2009)
14. H.-W. Liao, Y.-F. Wang, X.-M. Liu, Y.-D. Li, Y.-T. Qian, *Chem. Mater.* **12** (2000)
15. M. Hojamberdiev, R. Kanakala, O. Ruzimuradov, Y. Yan, G. Zhu, Y. Xu, *Opt. Mater.* **34**, 1954 (2012)
16. M.L. DosSantos, R.C. Lima, C.S. Riccardi, R.L. Tranquilin, P.R. Bueno, J.A. Varela, E. Longo, *Mater. Letters* **62**, 4509 (2008)
17. M. Zawadzksi, *J. Alloys Compd.* **451**, 595 (2008)
18. Y. Ma, L. Qi, *J. Colloid Interface Sci.* **335**, 151 (2009)
19. K. Polak, M. Niki, K. Nitsch, M. Kobayashi, M. Ishii, Y. Usuki, *J. Jarolimerk, J. Lumin.* **781** (1997)
20. O.V. Rzhetskaya, D.A. Spasskii, V.N. Kolobanov, V.V. Mikhailin, L.L. Nagornaya, I.A. Tupitsina, B.I. Zadneprovskii, *Opt. Spectrosc.* **104** (2008)
21. Y.A. Hizhnyi, S.G. Nedilko, T.N. Nikolaenko, *Nucl. Instrum. Methods Phys. Res. A* **537**, 36 (2005)
22. Y.C. Kong, D.P. Yu, B. Zhang, W. Fang, S.Q. Feng, *Appl. Phys. Lett.* **78**, 407 (2001)
23. R. Chen, G.Z. Xing, J. Gao, Z. Zhang, T. Wu, H.D. Sun, *Appl. Phys. Lett.* **95** (2009)
24. C.S. Lim, *Mater. Chem. Phys.* **131**, 714 (2012)
25. D. Son, D.-R. Jung, J. Kim, T. Moon, C. Kim, B. Park, *Appl. Phys. Lett.* **90** (2007)
26. B. Gao, H. Fan, X. Zhang, *S. Afr. J. Chem.* **65**, 125 (2012)
27. D. Modi, M. Srinivas, D. Tawde, K.V.R. Murthy, V. Verma, N. Patel, *J. Exp. Nanosci.* (2014). doi:[10.1080/17458080.2014.899714](https://doi.org/10.1080/17458080.2014.899714)